

# Horizontal prion transmission in mule deer

The gathering of deer during winter may foster the spread of chronic wasting disease.

Epidemics of contagious prion<sup>1</sup> diseases can be perpetuated by horizontal (animal to animal) and maternal (dam to offspring, before or after birth) transmission<sup>2–7</sup>, but the relative importance of each mechanism is unclear. Here we compare the incidence of chronic wasting disease (CWD) in captive mule deer (*Odocoileus hemionus*) that is attributable to horizontal or maternal transmission. We find that horizontal transmission is remarkably efficient, producing a high incidence of disease (89%) in a cohort of deer in which maternal transmission was improbable. Our results indicate that horizontal transmission is likely to be important in sustaining CWD epidemics.

Although prion diseases have emerged worldwide as a threat to human and animal

health, they are incompletely understood. Of those recognized so far in mammalian species (including humans), only scrapie and CWD behave as contagious diseases; however, their control is impeded by a lack of basic knowledge about the transmission of the infective prion agent. Horizontal transmission apparently drives scrapie epidemics in sheep<sup>3,5,6</sup>, but genetics also influence these patterns<sup>5</sup>. The epidemiology of CWD in mule deer resembles that of scrapie<sup>7</sup>, but the susceptibility of deer to the disease does not seem to be affected by genotype<sup>8</sup>.

It follows that CWD in mule deer (Fig. 1) represents a simple system for studying the mode of transmission of a contagious prion disease. We therefore compared the relative contribution of horizontal and maternal transmission of CWD in this species over a 5-year period (1997–2002). Captive mule deer in Colorado wildlife research facilities have been infected with CWD since the 1960s<sup>4</sup>. After attempts to eradicate CWD from the Foothills Wildlife Research Facility (FWRF) of the Colorado Division of Wildlife in 1985 (ref. 4), a new mule deer herd was started in 1990 with nine founders and augmented with fawn cohorts raised in 1991, 1992, 1993 and 1994. Despite preventive measures, CWD was diagnosed in 1994 in an FWRF-born female from the 1991 cohort. By May 1997, 10 cases had occurred among 57 resident deer (Fig. 2a).

We compared CWD incidence (defined as the number of animals affected divided by the number of animals at risk) in two sympatric mule deer cohorts. One cohort (R) of 10 deer was born to FWRF-resident dams in June 1997. Because the dams of all except one R-cohort deer eventually contracted CWD, maternal transmission was a possibility in this cohort.

The other cohort (NR) of 11 deer was also born in June, but away from the FWRF, and was added to the FWRF population in September–October 1997. Tonsil biopsies were negative in these NR deer, who were weanling fawns of about 3.5 months old that had been randomly captured from an enclosed, geographically separate herd in which CWD has not been detected (0 positive results out of 198 samples from deer aged one year or older, evaluated post mortem by immunohistochemistry of brain and lymphoid tissues; the 95% confidence interval for prevalence in this source herd was 0–1.9%). We presumed that dams of NR deer were not infected with CWD.

A comparison of these two cohorts shows that maternal transmission made little, if any, contribution to the occurrence of CWD.



**Figure 1** Close quarters: proximity with fellow deer seems to be the overriding factor in the spread of chronic wasting disease.

Despite the difference in potential for neonatal exposure to the disease, the overall CWD incidence was similar (Fisher's exact test,  $P \approx 1.0$ ) in the R and NR cohorts: 9 out of 9 R individuals surviving for 1.8 years or longer developed CWD, as did 8 out of 9 NR individuals surviving for this length of time. The relative risk of CWD infection in R deer was 1.1 (95% confidence interval, 0.9–1.4).

Mean intervals to CWD-caused death did not differ ( $z = -1.07$ ,  $P = 0.28$ ) between the R and NR cohorts, but the dynamics of the epidemic differed slightly (Kaplan–Meier  $\chi^2 = 3.74$ , d.f. = 1,  $P = 0.053$ ; Fig. 2b). This could be due partly to the differing ages at initial exposure for the two cohorts, an effect that is seen in scrapie<sup>3,5</sup>.

Further evidence of horizontal transmission<sup>6,9</sup> was provided by the increase in the cohort-specific incidence of CWD and the sharp decrease in the mean age of death from CWD in the FWRF herd (Fig. 2c).

The accumulation of abnormal prion protein in the peripheral lymphatic tissue of a host species seems to be strongly related to the horizontal transmissibility of prion diseases, and so might be a better predictor of contagiousness than the prion strain itself. The demonstration of abnormal prion protein in gut-associated lymphoid tissues<sup>10,11</sup> but not in placental tissues<sup>11</sup> of mule deer infected with CWD is consistent with an alimentary shedding route<sup>8</sup>, as has been suggested for scrapie<sup>12</sup>.

Both direct and indirect transmission of CWD can probably occur<sup>8</sup>, and concentrating deer in captivity or by feeding them artificially may facilitate transmission. The social behaviour of deer, particularly their tendency to gather and yard together during winter, might also foster epidemics in the wild. The efficiency of horizontal CWD transmission, exacerbated by behavioural ecology, might explain the high probability of CWD's becoming established in deer populations once it has been introduced either by natural spread or by the commercial movement of infected animals.

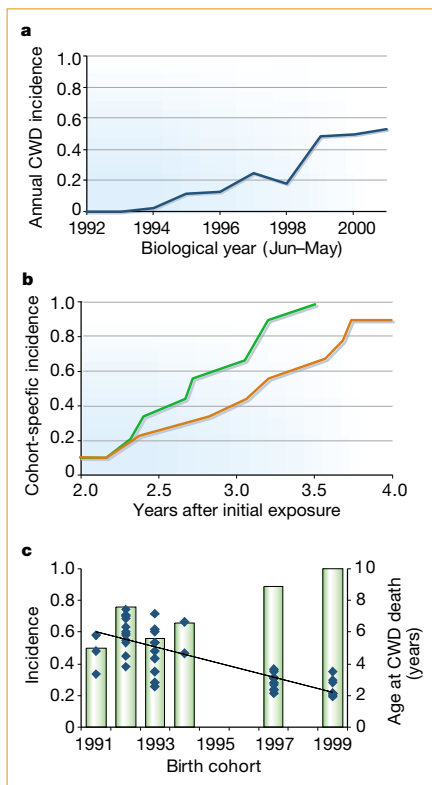


**Figure 2** Horizontal transmission of chronic wasting disease (CWD) in captive mule deer. **a**, Annual incidence of CWD increased from 1994 to 2001. **b**, The cumulative incidence of CWD in deer in the R cohort (born to a CWD-infected dam; 100%; green line) and in the NR cohort (born to an uninfected dam; 89%; orange line) is similar, but the forms of the epidemic curves differ slightly. Deaths from CWD in R and NR deer occurred at  $2.8 \pm 0.2$  years (range, 2.2–3.5 years) and  $3.1 \pm 0.2$  years (range, 2.1–3.7 years) after exposure, respectively. **c**, Cohort-specific incidence (bars) increases and age at CWD-caused death declines ( $-0.46 \text{ yr}^{-1}$ ;  $P < 0.001$ ; diamonds) in 1991–99, which is consistent with horizontal transmission<sup>6,9</sup>. No data are shown for 1995, 1996 or 1998 because fawns were not recruited in those years (c).

M. MILLER

Michael W. Miller\*, Elizabeth S. Williams†

\*Colorado Division of Wildlife, Wildlife Research Center, Fort Collins, Colorado 80526, USA  
e-mail: mike.miller@state.co.us

†Department of Veterinary Sciences, University of Wyoming, Laramie, Wyoming 82070, USA

1. Prusiner, S. B. *Proc. Natl Acad. Sci. USA* **95**, 13363–13383 (1998).
2. McFadyean, J. J. *Comp. Pathol. Ther.* **31**, 102–131 (1918).
3. Hourrigan, J., Klingsporn, A., Clark, W. W. & de Camp, M. in *Slow Transmissible Diseases of the Nervous System: Vol. 1* (eds Prusiner, S. B. & Hadlow, W. J.) 331–356 (Academic, New York, 1979).

4. Williams, E. S. & Young, S. *Rev. Sci. Tech. Off. Int. Epiz.* **11**, 551–567 (1992).
5. Hoinville, L. J. *Rev. Sci. Tech. Off. Int. Epiz.* **15**, 827–852 (1996).
6. Woolhouse, M. E. J., Stringer, S. M., Matthews, L., Hunter, N. & Anderson, R. M. *Proc. R. Soc. Lond. B* **265**, 1205–1210 (1998).
7. Miller, M. W. *et al. J. Wildl. Dis.* **36**, 676–690 (2000).
8. Williams, E. S. & Miller, M. W. *Rev. Sci. Tech. Off. Int. Epiz.* **21**, 305–316 (2002).
9. Redman, C. A. *et al. Epidemiol. Infect.* **128**, 513–521 (2002).
10. Sigurdson, C. J. *et al. J. Gen. Virol.* **80**, 2757–2764 (1999).
11. Spraker, T. R. *et al. Vet. Pathol.* **39**, 110–119 (2002).
12. Hadlow, W. J., Kennedy, R. C. & Race, R. E. *J. Infect. Dis.* **146**, 657–664 (1982).

Competing financial interests: declared none.

Nanotube electronics

## Large-scale assembly of carbon nanotubes

Nanoscale electronic devices made from carbon nanotubes, such as transistors and sensors<sup>1–5</sup>, are much smaller and more versatile than those that rely on conventional microelectronic chips, but their development for mass production has been thwarted by difficulties in aligning and integrating the millions of nanotubes required. Inspired by biomolecular self-assembly processes, we have created chemically functionalized patterns on a surface, to which pre-grown nanotubes in solution can align themselves in huge numbers. This method allows wafer-scale fabrication of millions of carbon-nanotube circuits with single-nanotube precision, and may enable nanotube-based devices, such as computer chips and high-density sensor arrays, to be produced industrially.

We used organic molecular marks on a substrate to guide the self-assembly of individual single-walled carbon nanotubes (swCNTs; see supplementary information). In the surface-functionalization step, we created two distinct surface regions coated either with polar chemical groups (such as amino (–NH<sub>2</sub>/–NH<sub>3</sub><sup>+</sup>) or carboxyl (–COOH/–COO<sup>–</sup>)) or with non-polar groups (such as methyl (–CH<sub>3</sub>)). We achieved this by direct deposition of proper organic molecules (for example, as a self-assembled monolayer) by dip-pen nanolithography<sup>6–8</sup> or by microcontact stamping<sup>9</sup>. These deposition techniques enabled us to functionalize the substrates without resorting to intermediate chemical steps, thereby minimizing surface contamination.

When the substrate is placed in a suspension of swCNTs, the nanotubes are attracted towards the polar regions and self-assemble to form pre-designed structures, usually within about 10 s. We used a magnet to remove common magnetic nanoparticle impurities from swCNT suspensions to improve the reliability of the process.

We discovered that a lateral-directional force exists on swCNTs near the boundary between the polar and non-polar molecular

regions (Fig. 1a). This force, which presumably originates from electrostatic interactions, rotates the swCNTs towards the polar region and confines them to the inside of it (Fig. 1a, inset).

Previous methods have relied on external forces, such as electric or magnetic fields, and liquid flow to align nanowires precisely<sup>10–13</sup>. However, it is time-consuming to align millions of randomly oriented nanotube circuits by using external forces. In our process, individual polar molecular marks attract and align swCNTs along pre-determined lines without external force, enabling any swCNT-based structure to be assembled simply by using polar molecular patterns with the required shapes.

We scaled up this process for high-throughput assembly. In principle, large numbers of microscale molecular patterns can easily be generated over a large chip area by using high-throughput patterning methods such as photolithography, stamping and, in the future, parallel dip-pen nanolithography<sup>8</sup>.

Our assembly of millions of individual swCNTs on stamp-generated microscale patterns that cover areas of about 1 cm<sup>2</sup> on gold, for example, occurs with a yield of more than 90% (Fig. 1b). Surprisingly, we found that in swCNT suspensions at low concentrations (for example, about 0.02 mg ml<sup>–1</sup> in

1,2-dichlorobenzene), only a single nanotube lies at the centre of each microscale polar molecular pattern, even though there is enough room for more nanotubes to assemble (Fig. 1b, inset). We used height profiles, determined by atomic-force microscopy, to confirm that assembly originated from one nanotube. Presumably, the hydrophobic surface of the swCNT passivates the polar pattern on the substrate and reduces the likelihood of adhesion by additional swCNTs.

We incorporated this process into conventional microfabrication methods to make millions of swCNT-based circuits over areas of about 1 cm<sup>2</sup>. Individual swCNTs are assembled between two polar molecular patterns generated by stamping on microfabricated gold electrodes. We used short (about 1 nm) polar molecules with π-electrons (such as 2-mercaptoimidazole) to minimize the contact resistance between the nanotubes and the electrodes. Atomic-force microscopy, using a conducting probe, confirmed the existence of stable swCNT circuits that conducted micro-ampere currents.

Figure 1c shows that more than 70% of the junctions are connected by only one swCNT. This proportion should increase as swCNT-purification processes advance or as the gap size is reduced for high-density integration (for example, a roughly 90% yield on flat surfaces). High-precision assembly should then enable swCNTs to be used in practical applications.

Saleem G. Rao, Ling Huang, Wahyu Setyawan, Seunghun Hong\*

Department of Physics, Center for Materials Research and Technology and Institute of Molecular Biophysics, Florida State University, Tallahassee, Florida 32306, USA

\*Present address: Department of Physics, Seoul National University, Seoul 151-742, South Korea  
e-mail: shong@phy.snu.ac.kr

1. Tans, S. J. *et al. Nature* **386**, 474–477 (1997).
2. Lee, J. *et al. Nature* **415**, 1005–1008 (2002).
3. Kong, J., Soh, H. T., Cassell, A. M., Quate, C. F. & Dai, H. *Nature*

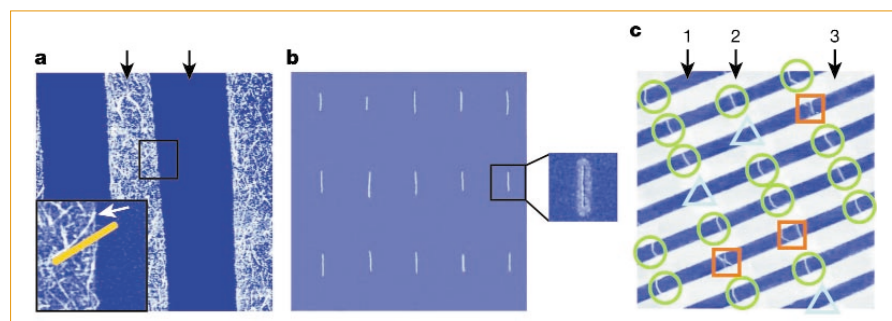


**Figure 1** Atomic-force micrographs showing large-scale self-assembly of single-walled carbon nanotubes (swCNTs). **a**, Image (12 × 12 μm<sup>2</sup>) showing the topography of swCNTs near the boundary (white arrow, inset) between polar (cysteamine; left arrow) and non-polar (1-octadecanethiol (ODT); right arrow) molecular patterns on gold. No swCNTs are evident in ODT regions. Yellow bar represents a tangent to a bent swCNT, showing the extent of bending due to lateral-directional force. **b**, Topography (30 × 30 μm<sup>2</sup>) of an array of individual swCNTs covering about 1 cm<sup>2</sup> of gold surface. The friction-force image (inset) shows a single swCNT (dark line), and the regions containing 2-mercaptoimidazole (bright area) and ODT (dark area). **c**, Topography (20 × 20 μm<sup>2</sup>) of an array of junctions with no swCNTs (triangles), one swCNT (circles) or two swCNTs (squares), covering an area of about 1 cm<sup>2</sup>. Arrows 1, 2 and 3 indicate octadecyltrichlorosilane (used to passivate the SiO<sub>2</sub> surface), 2-mercaptoimidazole on gold, and ODT on gold, respectively.